Artical ID:1006-3471(2012)06-0479-17

Advances and Challenges of Intermediate Temperature Solid Oxide Fuel Cells: A Concise Review

Sanping Jiang*

(Fuels and Energy Technology Institute, Department of Chemical Engineering, Curtin University, Perth, WA 6102, Australia)

Abstract: Fuel cell is an electrochemical energy conversion device to directly convert the chemical energy of fuels to electricity. Among all types of fuel cells, solid oxide fuel cells (SOFCs) operating at intermediate temperatures of 600 ~ 800 ℃ offer an attractive option that is much more fuel flexible than low temperature fuel cells such as proton exchange membrane fuel cells, and is suitable for a wide range of applications. However, two main challenges remain towards the commercial viability and acceptance of the SOFC technologies: the cost and durability. Both are critically dependent on the process, fabrication, performance, chemical and microstructural stability of various cell components, including anode, cathode, electrolyte, interconnect, and seal. Manifold and balance of plant materials also need to be carefully selected to ensure the structural stability and integrity with minimum volatile species. This article aims at providing a concise review and outlook of materials and components that have studied for SOFCs. The opportunities and challenges for the new generation of SOFCs technologies are briefly discussed.

Key words: intermediate temperature solid oxide fuel cells; review; challenges; materials

CLC Number: TM911.4 **Document Code:** A

1 Introduction

The demand for clean, secure and sustainable energy sources has simulated great interests in electrochemical energy storage and conversion technologies such as advanced batteries, fuel cells and supercapacitors. Among them, fuel cell is particularly attractive as fuel cell is considered to be the most efficient, and less polluting power-generating technology. Fuel cell is an electrochemical device that directly converts the chemical energy of fuels such as hydrogen, natural gas, methanol, ethanol and hydrocarbons to electricity and is a potential and viable candidate to moderate the fast increase in power requirements and to minimize the impact of the increased power consumption on the environment. Fuel cells are also versatile devices ranging from low temperature (<100 ℃) fuel cells such as alkaline fuel cells (AFC) and proton exchange membrane fuel cells (PEMFCs) to high temperature (500 ~ 1000 ℃) molten carbonate fuel cells (MCFCs) and solid oxide fuel cells (SOFCs). Among all types of fuel cells, SOFCs offer great promise for the most efficient utilization of various readily available carbon-containing fuels such as natural gas, hydrocarbons, gasified coal and solid carbon. For stand-alone applications, chemical to electrical efficiency of a SOFC is 45 to 65%, based on the lower heating value (LHV) of the fuel, which is twice that of an internal combustion engine.

A SOFC consists of a porous anode, a fully dense solid electrolyte, and a porous cathode. Driven by the differences in oxygen chemical potentials, oxygen ions migrate through the electrolyte to the anode where they are consumed by oxidation of fu-

Received: 2012-05-31, Revised: 2012-07-26 *Corresponding author, Tel: +61 8 9266 9804, E-mail: s.jiang@curtin.edu.au
The financial support by Australia Research Council under contract LP110200281 and National Natural Science Foundation of China (U1134001) is greatly acknowledged.

els such as hydrogen, methane and hydrocarbons (C_nH_{2n+2}). Fig. 1 illustrates the operation principle of a SOFC.

The state-of-the-art SOFCs are based on yttria-stabilized zirconia (YSZ) electrolyte, lanthanum strontium manganite ($La_{1-x}Sr_xMnO_{3-\delta}$, LSM) or lanthanum strontium cobalt-iron ($La_{1-x}Sr_xCo_{1-y}Fe_xO_{3-\delta}$, LSCF) perovskite oxide cathodes and nickel-YSZ cermet anode. Traditional SOFCs operate at 1000 ℃, because of the relatively low oxygen ion conductivity and high activation energy of oxide electrolytes such as YSZ. However, the high operating temperature is a key technical issue that has limited the development and wide deployment of this technology due to high system cost, high performance degradation rate, slow start-up and limited shutdown-startup cycles. Lowering of the operating temperature of SOFCs to intermediate range of 600 ~ 800 ℃ brings substantial technical and economic benefits due to wider materials selections for interconnect and compressive nonglass/ceramic seals, as well as reduced balance of plant (BOP) costs. However, reduction in operation temperature results in a significant increase in the electrolyte and electrode resistivity and the polarization losses. To compensate for the performance losses, the thickness of electrolyte layer has to be reduced in order to lower the ohmic resistance of the cell. Using a thin electrolyte layer, the electrolyte can no longer mechanically support the cell. Thus, electrode-supported cells, typically anode-supported cells have been developed. The oxygen reduction reaction on the cathode is the most sluggish reaction when the temperature is reduced to < 800 ℃[1]. Thus, the development of highly active and stable cathodes for IT-SOFCs is also one of the main tasks at the intermediate temperature region. There are significant activities in the research and development in the materials, fabrication technologies and stack designs for intermediate temperature SOFCs, or IT-SOFCs[1-2]. This article aims to provide a concise review of the current status, advances and challenges of IT-SOFCs technologies.

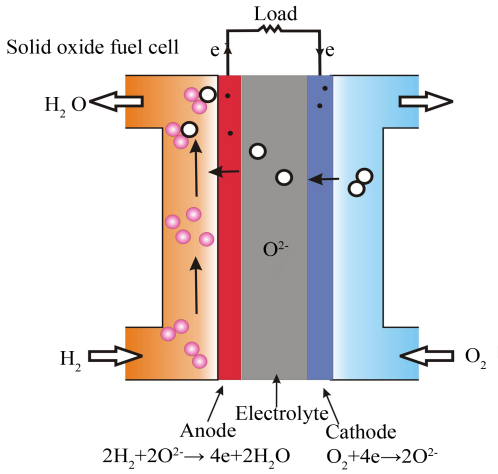

Fig. 1 Schematic representation of operating principle of a solid oxide fuel cell.

2 Development of Key Materials

2.1 Anode and Cathode

Anode: For SOFCs based on YSZ electrolyte, metal-ceramic composite cermet, especially Ni/YSZ or Ni/gadolinia-doped ceria (Ni/GDC) cermets, are the most commonly used anodes[3]. The function of the oxide component is primarily to reduce the sintering of the Ni metal phase, to decrease the thermal expansion coefficient (TEC) and to improve the electrochemical performance of the anode. Thus, the composition and phase distribution are important for the thermal, electrical and ionic conductivity properties, microstructure and performance of the anodes. For example, with addition of 30% (by volume) YSZ, the TEC of the Ni/YSZ cermet is ~ 12.5×10^{-6} K^{-1}, which is close to that for the YSZ electrolyte[4]. The electrical conductivity of typical Ni/YSZ cermet (with a volume ratio of YSZ to Ni of 40∶60 and porosity of 30 ~ 40%) is in the range of 102 to 103 $S\cdot cm^{-1}$. For a simple two-phase system the theory predicts the percolation threshold at ~ 30 % (by volume) of the phase with higher conductivity for the transition from dominant ionic conductivity to dominant electronic conductivity[5]. Adding electrochemically active and mixed conducting interlayer, such

as yttria-doped ceria (YDC) between anode and electrolyte was shown to significantly reduce the electrode polarization resistance for methane oxidation on Ni/YSZ anode[6].

An important issue regarding the Ni-based cermet anodes is the microstructure degradation under SOFC operating conditions. The predominant microstructure change is agglomeration and coarsening of the Ni phase, primarily due to the poor wettability between the metallic Ni and YSZ oxide phase[7]. At SOFC operation temperatures, coarsening kinetics is fast and agglomeration of Ni occurs relatively rapidly[8]. Focus ion beam-scanning electron microscopy (FIB-SEM) technique is particularly useful in obtaining three dimensional phase distribution in SOFC electrodes to study the microstructure change of the electrodes[9-10]. Fig. 2 shows the simulated microstructural evolution of Ni-YSZ anode functional layers using phase-field approach[10]. The simulations assumed that the YSZ phase did not change whereas the Ni phase was allowed to coarsen via Ni surface diffusion. An experimentally obtained three-dimensional reconstruction of a functional layer from an anode-supported SOFC is used as the initial microstructure. The evolution of the microstructure is characterized by examining the three phase boundary (TPB) density, interfacial area per unit volume, and tortuosity versus time. Considerable coarsening, as well as smoothening of surfaces, is evident comparing the results in Fig. 2.

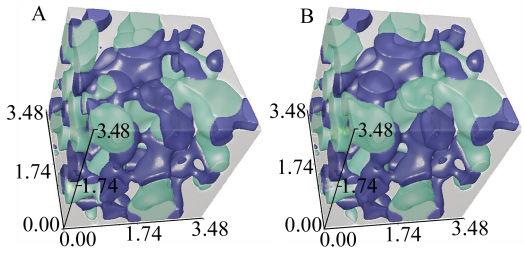

Fig. 2　3D image renderings of a Ni/YSZ anode functional layer in the as-prepared state (A) and after coarsening using a phase-field model (B) (Light color represents Ni, Deep color represents pore, and the YSZ phase is transparent)[10].

Carbon deposition and sulfur poisoning are two of the major issues facing the long-term stability and practical applications of SOFC technologies based on direct utilization of hydrocarbon fuels ranging from natural gas to diesel in which the most abundant impurity is sulfur. Sulfur is a major impurity in coal, so sulfur tolerance is also a major issue for SOFC power plants designed to utilize gasified coal. Ni/YSZ based cermet anodes have a very limited tolerance to H_2S. As shown by Zha et al., the sulfur poisoning is generally characterized by a two-stage behavior: a rapid drop in the cell performance upon exposure to H_2S, followed by a gradual but persistent deterioration in performance[11]. Nickel and alloys based metals are highly active for carbon cracking and deposition of carbon can result in the blocking of the active sites and disintegration of bulk metals and alloys into metal particles at high temperatures (300 ~ 850 ℃). The carbon cracking can be avoided by providing a high enough steam to carbon (S/C) ratio in the fuel gas, e.g., by mixing the fuel with H_2O[12]. However, high S/C ratio is not attractive for fuel cells as it lowers the electrical efficiency of the fuel cells by diluting the fuel. The endothermic nature of the steam reforming reaction can also cause local cooling and steep thermal gradients potentially capable of mechanically damaging the cell stack. Thus, development of anodes with high tolerance towards carbon deposition and sulfur poisoning is critical for SOFCs utilizing hydrocarbon fuels.

Replacing Ni with carbon-inert Cu to form Cu/YSZ cermet anodes[13] and using Ni-Cu/YSZ cermet anodes prepared by impregnation of porous YSZ layer with copper and nickel nitrate solution[14] were found to improve the resistance towards carbon deposition. One main issue with Cu-based cermet anodes is the microstructure instability of copper phase. A number of groups have shown that perovskite oxides, e.g., $(La,Sr)(Cr,Mn)O_3$ (LSCM) and $(La,Sr)VO_3$ (LSV), exhibit better sulfur tolerance[15-18]; LSV makes it possible to work with >10% H_2S in the fuel[17]. Unfortunately, LSV appears

to be insufficiently stable for use in SOFCs. Recently Yang et al reported the development of a composite anode consisting of $Pr_{0.8}Sr_{1.2}(Co,Fe)_{0.8}Nb_{0.2}O_{4+\delta}$ scaffold with homogeneously dispersed nano-sized Co-Fe alloy, showing good performance with high sulfur tolerance and coking resistance[19]. One of the main concerns of the ceramic oxide based anodes is their generally low electronic conductivity as compared to metallic Ni [20-21]. In the case of LSCM, the electrical conductivity is 38 $S\cdot cm^{-1}$ in air at 900 ℃ and drops significantly to 5 $S\cdot cm^{-1}$ in 5% H_2[22]. The poor electrical conductivity can lead to the significant increase in the electrode ohmic and polarization resistance and contact resistance between the electrode coatings and current collector [23].

Many methods have been investigated to modify Ni-based materials to enhance the sulfur-tolerance and carbon cracking resistance for direct utilization of hydrocarbon fuels. Replacing YSZ with doped ceria in the Ni-based cermet also enhances the electrocatalytic activity towards oxidation of hydrocarbon fuels and sulfur-tolerance due to the redox transition between Ce^{4+}/Ce^{3+} mixed valent cation [24-25]. Impregnation or infiltration of nano-sized electrocatalysts such as doped ceria, Pd, and a proton-conductor $SrZr_{0.95}Y_{0.05}O_3$ has shown some success, since the introduced nano-sized electrocatalysts can significantly promote the electrochemical activity of conventional Ni-based anodes towards the oxidation of hydrogen and hydrocarbon fuels and suppress carbon cracking and sulfur poisoning[26-29]. Infiltration of GDC nanoparticles in Ni/YSZ cermet anodes showed the significantly improved electrode performance and stability in methane without causing carbon deposition [30]. Most recently Yang et al showed that introducing barium oxide nanoparticles drastically increase the carbon tolerance in dry C_3H_8 by promoting water-mediated carbon removal (see Fig. 3[31]). Surface modification of existing Ni-based cermet anodes remains an attractive option for the significant enhancement of sulfur and carbon tolerance without comprising performance[32].

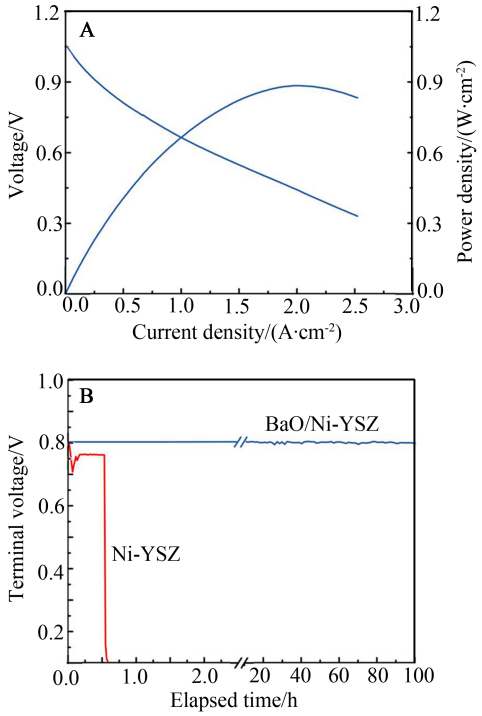

Fig. 3 Current-voltage characteristics and the corresponding power densities measured at 750 ℃ for cells with a configuration of BaO/Ni-YSZ|YSZ|SDC/LSCF when dry C_3H_8 was used as the fuel and ambient air as the oxidant (A), and Terminal voltages measured at 750 ℃ as a function of time for the cells with and without BaO/Ni interfaces operated at a constant current density of 500 $mA\cdot cm^{-2}$ with dry C_3H_8 as the fuel (B) (water was formed on the anode by electrochemical oxidationof dry C_3H_8)[31].

Cathode: LSM is still the materials of choice for cathodes of SOFCs with YSZ electrolytes [33]. LSM shows a high thermal stability and compatibility with YSZ; more important, if compared to other cathode materials, LSM has an excellent microstructural stability and its long-term performance stability has been well established. However, LSM is predominant electronic conductor with negligible oxygen ion conductivity. As the incorporation and bulk diffusion of oxygen inside LSM cannot be expected to occur to a significant degree[34], the O_2 reduction reaction sites primarily

occur at TPB areas, which becomes a limiting factor for the application of LSM cathode for SOFC operation at intermediate temperatures of 600 ~ 800 ℃. Various strategies have been developed to improve the electrocatalytic activity of the LSM-based cathodes. For example, addition of YSZ phase to LSM significantly reduced the electrode polarization resistance[35]. The electrochemical performance of a LSM cathode can also be enhanced substantially by introducing catalytically active nanoparticles, such as doped CeO_2, into the LSM porous structure[36].

LSCF-based perovskites with compositions $La_{0.6}Sr_{0.4}Co_{0.2}Fe_{0.8}O_3$ or LSCF6428 may have desirable properties for IT-SOFC cathode applications and has been extensively studied[37]. Acceptor-doped cobaltites are characterized by enhanced lattice oxygen vacancy formation and, hence high ionic conductivity. The oxygen self-diffusion coefficient of cobaltite based materials is several orders of magnitude higher than that of the manganites[34]. Fig. 4 shows a comparison of polarization performance of LSM and LSCF cathodes measured in air under identical conditions[38]. LSCF shows a much higher activity towards oxygen reduction reaction as compared to that on LSM. The main hurdles with the Co-rich perovskite oxides is the high TECs (~16-18×10^{-6} K^{-1}) and high chemically activity with YSZ electrolytes. Replacing lanthanum with barium at the A-site of LSCF substantially enhances its electrochemical activity for the O_2 reduction reaction at intermediate temperatures. Shao and Haile[39] applied $Ba_{0.5}Sr_{0.5}Co_{0.8}Fe_{0.2}O_3$ (BSCF) as cathode to a doped ceria electrolyte cell and achieved the power densities of 1.01 W·cm^{-2} and 402 mW·cm^{-2} at 600 ℃ and 500 ℃, respectively, when operated with hydrogen as the fuel and air as the cathode gas. However, its high TEC (~ 20×10^{-6} K^{-1}[40]), low electrical conductivity (~ 25 S·cm^{-1} at 800 ℃[40]) and instability in air[41] are some of the challenges for the practical application of BSCF cathodes in SOFCs. Coating a CO_2-protective shell by infiltration of conductive and stable La_2NiO_4 to BSCF porous scaffold was shown to be effective to substantially enhance the

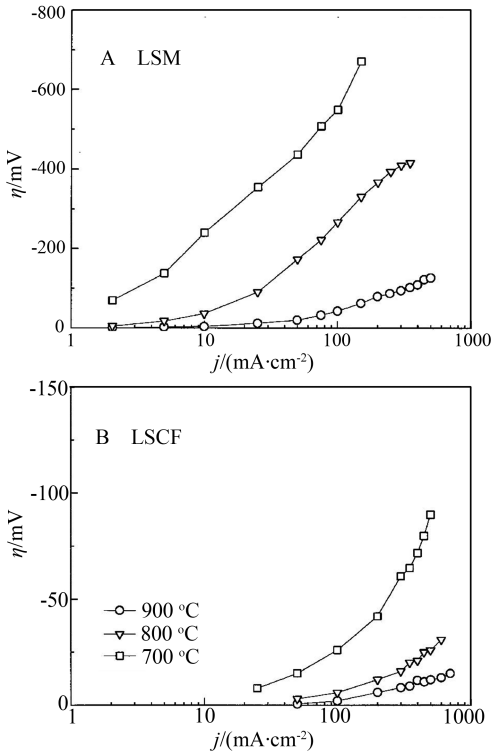

Fig. 4　Steady state polarization curves of LSM (A) and LSCF (B) electrodes measured at different temperatures in air[38].

resistance of the BSCF cathode towards CO_2 attack[42].

Cathode can be gradually degraded and deactivated by contaminants such as chromium, sulfur, boron which can be either in the air stream or from the volatile species of cell components, such as metallic interconnect, sealant and manifold[43-45]. Chromium deposition and poisoning on SOFC cathodes have been extensively investigated and are due to the fact that the gaseous chromium species from the chromia-forming metallic interconnect migrate through the cathode and deposit in the form of low valence chromium(III) species either at the electrode/electrolyte interface, inside the bulk of the electrode and/or on the electrode surface. The accumulation of Cr deposits poisons and leads to irreversible polarization losses of the cathode and performance degradation of the cell[44, 46-51]. Compared to chromium, deposition and poisondue to the source of sulfur and boron contaminants is not as well recognized as that of chromium from chromia-forming

alloys. The presence of impurities such as volatile species (Na, B, etc.) from ceramic-glass seals and sulphur or other minor elements such as Si and Al can have serious degradation effect on the cathode of SOFC [52-55]. The impurities in the air stream may not be avoidable due to the multi-components and multi-processes involved in the synthesis and fabrication of stacks; therefore it is critical to develop cathodes with not only the high activity but also the high tolerance towards impurities and contaminants in air stream.

2.2 Nanoscale and Nanostructured Electrodes

The nanoscale and nano-structured electrode approach by impregnation or infiltration method attracts increasing attention as the viable alternative for the development of new electrodes for IT-SOFCs[56-59]. Infiltration method is a two-step sintering process, which effectively separate the catalytic active phase formation temperature from the high sintering temperature as required to establish the intimate electrode/electrolyte interface bonding in the standard SOFC electrodes. The relatively low formation temperatures (< 700 ~ 800 ℃) for the catalytic active phases minimizes the grain growth and agglomeration, resulting in the deposition of nano-sized particles onto structurally stable and compatible scaffolds such as LSM, Ni/YSZ, and YSZ or doped ceria. The infiltration method opens a new horizon in the electrode development as the method expands the selection of variable electrode materials combinations with the minimized TEC mismatch and the suppression of possible detrimental reactions between electrode and electrolyte materials.

Fig. 5 shows the scheme of nano-structured electrodes by two-step infiltration route[56]. The infiltrated catalytic nanoparticles can form discrete distribution or a thin and continuous network on the surface of the porous scaffold. The porous scaffold can be electronic conducting electrode materials such as LSM or ionic conducting electrolyte materials such as YSZ and doped ceria. The latter requires deposition of a continuous nanoparticle layer with high electronic conductivity as well as high electrocatalytic activity, and multiple infiltration steps are necessary to achieve sufficient electron conduction[60]. Such repeated infiltration process is time-consuming and hinders the practical application of the infiltration approach. Using a concentrated LSM nitrate precursor solution with surfactant (e.g.,Triton-X 100), Sholklapper et al showed that it may be possible to form a continuous LSM nanoparticles on YSZ scaffold with a single-step infiltration [59,61]. However, from practical point of view, it would be very difficult for concentrated precursor solutions to penetrate and infiltrate uniformly into micro- and nanopores of the scaffold by capillary force, and multiple infiltration-calcination steps are generally required, particularly in the case of thick anode-substrate supports. On the other hand, the infiltration process can be accelerate by electrodeposition and electroless deposition methods[62-63].

The enhancement in the electrochemical performance of nanostructured electrodes is truly remarkable. For instance, Jiang et al showed that in the case of LSM cathodes, the electrode polarization resistance (R_E) is 11.7 Ω·cm^2 at 700 ℃. With the infiltration of 5.8 mg·cm^{-2} GDC nanoparticles, R_E is reduced dramatically to 0.21 Ω·cm^2, which is 56 times smaller than that of the pure LSM cathode at the same temperature[64]. The R_E for the O_2 reduction reaction on the nano-structured Pd+YSZ is 0.11 Ω·cm^2 at 750 ℃ and 0.22 Ω·cm^2 at 700 ℃, and this is significantly lower than that of the LSM (9 to 54

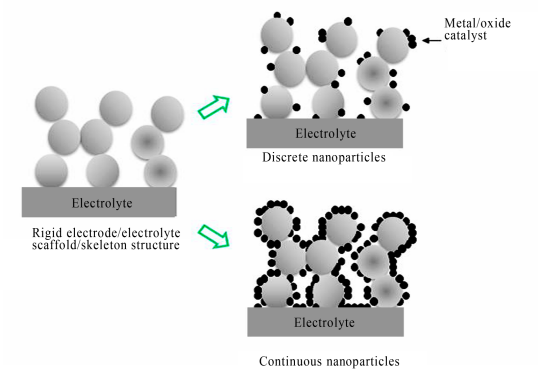

Fig. 5 Scheme of the infiltrated nano-structured electrodes onpre-sintered porous electrode or electrolyte scaffold/skeleton[56].

Ω·cm² at 700 ℃ [65-66]), LSM/YSZ (2.5 Ω·cm² at 700 ℃[67]) and LSM/GDC (1.1 Ω·cm² at 700 ℃[65]) composite cathodes. The most distinctive advantage of the nanostructured approach is the flexibility in the selection and combination of highly active catalytic materials with structurally stable and highly electronic or ionic conducting scaffold to meet stringent requirements of anodes and cathodes of SOFCs. For example, the high performance SOFC cathodes can be developed by the combination of highly active MIEC but thermally incompatible materials such as BSCF with the structurally stable and highly conductive LSM scaffold. In such nanostructured BSCF-infiltrated LSM composite cathode, the uniformly distributed BSCF nanoparticles significantly enhance the electrochemical activity, while the LSM scaffold provides an effective electron transfer path, TEC matching and thermal stability with the YSZ electrolyte. The interfacial reaction between the infiltrated BSCF and YSZ is minimized due to the low phase formation temperature of BSCF. Fig. 6 shows the performance of anode-supported YSZ film cells with pure LSM and 1.1 mg·cm^{-2} BSCF-infiltrated LSM cathodes at different temperatures under H_2/air[68]. The cell with thin YSZ electrolyte film and the nanostructured BSCF-LSM cathode exhibits maximum power densities of 1.21 and 0.32 W·cm^{-2} at 800 ℃ and 650 ℃, respectively, substantially higher than 0.51 and 0.08 W·cm^{-2} for the cells with the pure LSM cathode under identical conditions.

The remarkable promotion effect of the nanostructured electrodes on the performance of anodes and cathodes of SOFCs is a direct result of the formation and uniform deposition of nano-sized and catalytically active phases on the surface of porous electrode or electrolyte scaffolds. Consequently, the most significant challenge in the application and development of nanostructured electrodes is the microstructure stability of the infiltrated nanoparticles. As the particle size of the infiltrated phase is very fine (20 ~ 100 nm), the tendency for sintering and

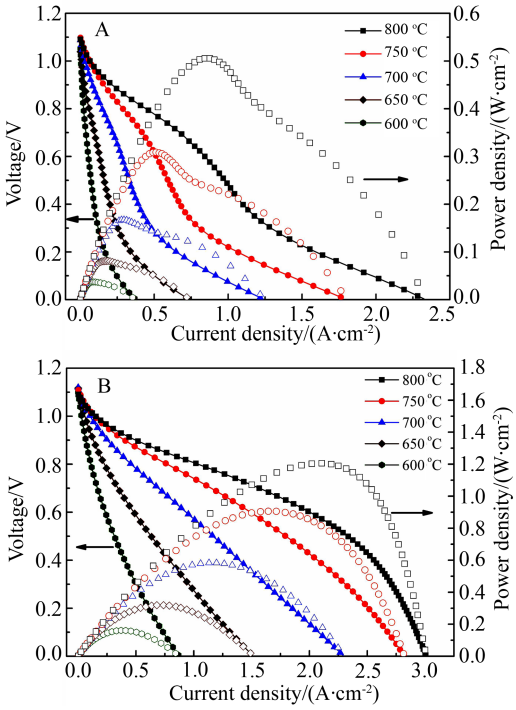

Fig. 6 Performance of the Ni/YSZ anode-supported YSZ electrolyte film cells with pure LSM cathode and (A) 1.1 mg·cm^{-2} BSCF-impregnated LSM composite cathode (B) atdifferent temperatures in H_2/air (H_2 flow rate: 200 mL·min^{-1}; oxidant: stationary air) [68].

grain growth at operation temperature of SOFCs (500 ~ 800 ℃) would be high due to the large surface energy associated with the nano-sized oxide or metallic phase[69]. In the case of infiltrated Pd nanoparticles on porous YSZ scaffold, the agglomeration and grain growth resulted in the formation of continuous and dense Pd films on the YSZ scaffold surface, leading to the increase in the polarization losses due to the blocking of the oxygen diffusion path[70]. Alloying with cobalt, manganese and silver has been found to increase the thermal stability and enhance the performance stability of Pd-infiltrated electrodes[70-71]. Reduction in operation temperature of SOFCs is expected to significantly benefit the microstructure stability of nanostructured electrodes.

2.3 Electrolytes

Any SOFC electrolyte must meet the requirements of fast ionic transport, negligible electronic conduction, and thermodynamic stability over a

wide range of temperature and oxygen partial pressure. In addition, they must have thermal expansion compatible with the electrodes and other cell components, good mechanical properties and negligible interaction with electrode materials under operation and processing conditions. The most common SOFC electrolyte is zirconia-based electrolyte materials, typically yttria-stabilized zirconia, because of its superior stability[72]. Although it is a good oxygen conductor, its conductivity is significantly lower than doped ceria and $LaGaO_3$ perovskites-based electrolytes (see Fig. 7[73]).

In the Y_2O_3-ZrO_2 system, a maximum of the conductivity of ZrO_2 electrolyte with respect to the dopant content occurs around 8 ~ 9% (by mole) Y_2O_3[74]. This maximum corresponds to the minimum dopant level required to fully stabilize the high-temperature cubic phase. Scandia-doped zirconia (ScSZ) provides a higher conductivity, attributed to the smaller mismatch in size between Zr^{4+} and Sc^{3+} ions [75]. ScSZ with 9.0% (by mole) Sc_2O_3 (9ScSZ) has the conductivity of 0.34 $S\cdot cm^{-1}$ at 1000 ℃[76]. The segregation of impurities such as silica[77] is detrimental, but can be improved by minor oxide additives[78].

Pure ceria is not a good oxygen ion conductor, but its conductivity can be increased significantly by substituting Ce^{4+} with divalent alkaline earth or

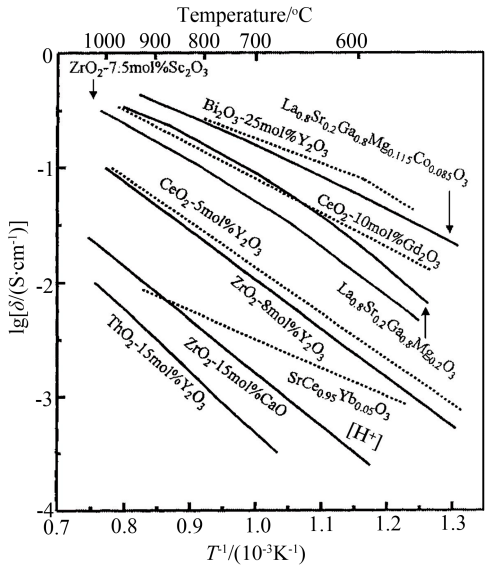

Fig. 7 Oxygen ion conductivity of selected electrolyte materials[73].

trivalent rare earth ions[79]. Highest conductivities have been reported for either Gd- or Sm-doped ceria (GDC and SDC) with the maximum conductivity obtained around 10 ~ 20 % (by mole) Gd_2O_3 or Sm_2O_3 [80-83]. Ceria-based electrolytes suffer from the partial reduction of Ce^{4+} to Ce^{3+}. However, the leakage current decreases substantially with the reduction in operation temperature[84].

Another major class of SOFC electrolyte materials is doped $LaGaO_3$ perovskites, in particular the lanthanum strontium magnesium gallate (LSGM) systems [73,85]. Ishihara et al. [86] fabricated 5-μm-thick $La_{0.8}Sr_{0.2}Ga_{0.8}Mg_{0.2}O_3$ thin electrolyte cells with 400-nm-thick $Gd_{0.2}Ce_{0.8}O_2$ interlayer by pulse laserdeposition, achieving maximum power density as high as 1.95 and 0.61 $W\cdot cm^{-2}$ at 600 ℃ and 500 ℃.

Tab. 1 lists the typical values of the oxygen ion conductivity and its activation energies in the low- and high-temperature ranges for the main electrolyte materials employed in SOFCs. Note that higher conductivity values are sometimes observed in thin films and other nanostructured systems. Kosacki et al.[87] investigated the ionic conductivity of highly textured YSZ films deposited on MgO substrate and observed exceptionally high ionic conductivity for film thickness < 60 nm. Recently Garcia-Barriocanal et al. [88] reported a huge ionic conductivity enhancement at interfaces of epitaxial YSZ/$SrTiO_3$ heterostructures. This indicates that nanoscale effects at the interface could be manipulated to enhance the ionic conductivity of zirconia-based electrolytes for low and intermediate temperature SOFC applications.

Apatite-type oxides with a general formula $(La/M)_{10-x}(Si/GeO_4)_6O_{2\pm\delta}$(M = Mg, Ca, Sr, Ba) are attracting considerable attention [89-90]. The ionic conductivity of $La_{10}Si_6O_{27}$ apatite electrolytes is 6.62×10^{-3} and 3.42×10^{-2} $S\cdot cm^{-1}$ at 600 and 800 ℃, respectively [91]. Though using modified gel-casting synthesis route can reduce the sintering and densification temperature slightly[91], its sintering and densification temperature is still too high (1650 ~ 1700 ℃)[92]. Bismuth oxide based materials, such as yttria and erbia-stabilized bismuth oxides, showed highest conductivities. For example, at 500 ℃, the resistance of erbia-stabilized bismuth oxides is reported to be

Tab.1 Conductivity and activation energy for some electrolyte materials employed in SOFCs

Composition (by mole)	E_a/eV		σ/(S·cm^{-1})		Ref.
	400 ~ 500 ℃	850 ~ 1000 ℃	1000 ℃	600 ℃	
3% Y_2O_3-97% ZrO_2	0.95	0.80	0.056		[72]
8% Y_2O_3-92% ZrO_2	1.10	0.91	0.16		[72]
10% Y_2O_3-90% ZrO_2	1.09	0.83	0.13		[72]
12% Y_2O_3-88% ZrO_2	1.20	1.04	0.068		[72]
9.0% Sc_2O_3-91% ZrO_2	1.30	0.72	0.34		[76]
$Gd_{0.2}Ce_{0.8}O_{1.9}$	0.86			16.9×10^{-3}	[82]
$Sm_{0.2}Ce_{0.8}O_{1.9}$	1.0			9.7×10^{-3}	[81]
$Y_{0.2}Ce_{0.8}O_{1.9}$	0.68			14×10^{-3}	[83]
$La_{0.8}Sr_{0.2}Ga_{0.8}Mg_{0.2}O_3$	0.63			17×10^{-3}	[73]

0.037 Ω·cm^2, 2 orders of magnitude lower than 1.259 Ω·cm^2 for YSZ at the same temperature[93]. The high oxygen mobility is a result of weak metal-oxygen bonds and thus Bi_2O_3-based materials have lower stability under reduced partial pressure of oxygen at the anode side, resulting in the decomposition to metallic Bi. However, the cell stability can be substantially improved by using functionally graded ceria/bismuth oxide bilayered structure[94]. A high power density of ~ 2 W·cm^{-2} at 650 ℃ was reported on an anode-supported cell with ceria/bismuth oxide bilayered structured electrolyte[95].

2.4 Interconnect and Sealant Materials

Alkaline-earth (AE)-doped $MCrO_3$ (M= La, Y and Pr) are the mostly studied ceramic interconnect materials for the high temperature SOFCs[96-97]. The increase in AE content results in a higher TEC, which causes thermal stresses and thus decreases long-term stability[98]. The praseodymium in $PrCrO_3$-based oxides exists in two valence states, Pr^{3+} and Pr^{4+}[99], which decreases chemical and dimensional stability. $La_{07}Ca_{03}CrO_3$-doped CeO_2 composite [100] and $Nd_{075}Ca_{025}Cr_{098}O_{3-\delta}$ [101] were also considered for interconnects. However, the decrease in their electrical and thermal conductivities with decreasing temperature is a major challenge in the developments of ceramic interconnect for IT-SOFCs.

Metallic materials based on transition metal-based oxidation resistant alloys have been considered to be the primary candidates as the interconnect materials of IT-SOFCs, due to the economic and easy processing benefits in addition to the high electrical and thermal conductivities. These include Ni(-Fe)-Cr based heat resistant alloys, Cr alloys, and chromia-forming ferric stainless steels[102-103]. The alloys with the formation of a protective and semi-conductive chromia scale to minimize further environmental attack during the high temperature operation and with TECs of 11.0 to 12.5×10^{-6} K^{-1} are the preferred candidates. The conductivity of chromia oxides is ~10^{-2} S·cm^{-1} at 800 ℃ in air[104]. A good example in this category is Plansee Ducralloy with a composition of 94% Cr, 5% Fe, and 1% Y_2O_3 (as $Cr_5FeY_2O_3$)[105]. To further increase the electrical conductivity of the scale and to reduce the chromium vaporization, a new alloy which contains 0.5% Mn (Crofer 22 APU) was developed[106]. The oxide scale consisted of a $(Mn,Cr)_3O_4$ spinel top layer shows a higher electrical conductivity [107].

However, without effective protective coatings, the vaporization of chromium species from chromia scale poisons the cathodes and seriously degrades the cell performance[44,46-51,108]. To reduce the growth rate of the oxide scale and the vaporization of chromium species, a thin and dense oxide coating with high electrical conductivity such as LSM and LSCo is often deposited on the metallic interconnect. The chromium

volatility can also be suppressed by modification of the metallic interconnect materials. Hua et al.[109] reported a novel Ni-Mo-Cr alloy with a TEC value of 13.92×10^{-6} K^{-1} between 35 and 800 °C. After oxidation treatment at 750 °C for 1000 h, the area specific resistance (ASR) of this alloy is 4.48 $m\Omega\cdot cm^2$. Poisoning study using LSM cathode indicates that the Cr deposition and poisoning of the Ni-Mo-Cr alloy is remarkably reduced as compared to the conventional Fe-Cr alloy[110].

The sealing material has been regarded as one of the most significant technical challenges in the development of planar SOFCs while sealing is much less of a problem for tubular SOFCs[111]. The sealants can be broadly classified into rigid bonded seals, compressive seals, and compliant bonded seals. Each offers advantages and limitations. In rigid bonded sealing, the sealant forms a joint that is non-deformable at room temperature. Because the final joint is brittle, it is critical for the sealant to match the TEC of the adjacent substrates. High temperature glass and ceramic-glass such as alkali silica glasses and $BaO\text{-}CaO\text{-}SiO_2$[112] are among the most important rigid bonded sealants employed in joining SOFC stacks. These materials have acceptable stability in the reducing and oxidizing atmospheres, are generally inexpensive, and can be readily applied to the sealing surfaces as a powder paste or a tape cast sheet. They are electrically insulating and their TEC can be adjusted to those of electrolyte and metallic interconnect. However, the brittle nature of glasses and ceramic-glasses makes these seals vulnerable to cracking, and they tend to transform in phases and react with the cell components and interconnect materials under SOFC operation conditions in a long run, due to their intrinsic thermodynamic instability[52, 113]. Recent results also show that volatile boron species from borosilicate glass has significant detrimental effect on the microstructure stability and electrochemical activity of nano-structured GDC-LSM cathodes of SOFCs[114].

Compressive seals have been developed to avoid the disadvantages of the rigid bonded seals, with the merit of flexibility and compressibility, allowing the cells and interconnects to expand and contract freely during thermal cycles and operation. This type of sealing relies on the compressive load of the stack. So far two kinds of compressive seals have been considered, i.e., the deformable metallic seals and the mica-based seals. The deformable metallic seals include ductile silver[115] and corrugated or C-shaped superalloy gaskets[116], but their application is limited due to their high electronic conductivity. The most common compressive sealing material is based on mica[117]. By incorporating a compliant interlayer such as a deformable metal or glass at the interface to form the hybrid mica-based seals, the sealing properties of mica are significantly improved[118-119]. Compliant bonded seals are based on metallic braze. Metallic materials have lower stiffness as compared to ceramics and can undergo plastic deformation, which allow for accommodation of thermal and mechanical stresses. Silver and gold are stable in air and are commonly used as metal braze materials[120]. A major challenge in obtaining a good metal-ceramic joint is adequate wetting of the ceramic by the braze metal. Comprehensive review articles have recently been published on sealant materials used for SOFCs[111,121].

3 SOFC Structures and Configurations

There are number of cell support structures and each is classified according to the layer that mechanically supports the cell. These include electrolyte-supported, anode- or cathode-supported as well as porous substrate- or metal-supported structures, see Fig. 8[2].

Due to the thick electrolyte (typically in the range of ~ 100 μm) needed to mechanically support other cell components, the electrolyte-supported SOFCs are primarily developed for operation at high temperatures (~ 900 °C or above)[122]. The rapid-progress in the thin-film technology[123], as well as the identification of alternative electrolyte materials with higher ionic conductivity such as GDC has significantly reduced the ohmic losses associated with solid elect rolyte. The use of thin electrolyte layers requires the electrolyte to be supported on an

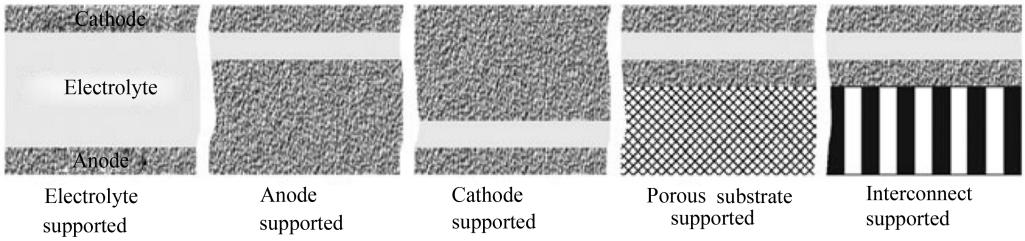

Fig. 8 Illustration of different types of cell support architec tures for SOFCs[2].

appropriate substrate. The substrates can be functional anode or cathode, or porous supports providing gas diffusion and transportation for fuel cell reactions. As the substrate is the principal structural component in these cells, it is necessary to optimize the conflicting requirements of mechanical strength and high gas permeability.

Up to now, the most popular supported cell structure is the anode-supported thin film SOFCs. The state-of-the-art anode-supported SOFC is based on porous Ni/YSZ cermets as a support. The anode support usually consists of a relatively thick porous supporting substrate (200～500 μm) and a thin and fine structured anodic function layer (AFL). To reduce the electrolyte ohmic resistance and to enhance the cell efficiency, the electrolyte layer deposited should be as thin as possible. As a general role, the film thickness is inversely proportional to the pore size and/or propagated roughness of the surface, which means that the larger the pore size, the more difficult it is to get a thinner electrolyte. Thus the AFL is also required to have proper pore structure with low surface roughness. Tape-casting and tape-calendering processes are the common techniques in the fabrication of anode-supported structure for thin film SOFCs[124-125]. Power density as high as 1.8 $W \cdot cm^{-2}$ at 800 ℃ was reported for such anode-supported cells [126]. However, the porous composite anode support is relatively weak mechanically and can have difficulty withstanding the thermal and mechanical stresses generated by rapid temperature fluctuation. Moreover Ni/NiO redox cycling induced by air diffusion into the anode compartment during the loss of fuel supply and other operational excursion can disrupt the anode microstructure, leading to performance degradation[127].

Metal-supported structures are often used to overcome the problems associated with anode-supported cells [128-129], in which the Ni/YSZ anode support is replaced by a metal (usually stainless steel). Metal support improves thermal shock resistance, reduces temperature gradients due to the high thermal conductivity of metals and thus enhances the robustness of SOFCs.

4 Conclusions

SOFCs have tremendous potential for numerous applications, from stationary to mobile power, with high fuel flexibility and high system efficiencies. However, common to all new and emerging technologies, cost and durability are two of the most technical barriers for the commercial viability and acceptance of the SOFC technologies. The high cost and low durability makes the fuel cells-based power systems not commercially competitive to existing conventional power generation technologies such as internal combustion engine and gas fired power plant. Though material costs would remain essentially constant, it is anticipated that the production costs will come down with volume. Fabrication process takes a lion's share of the cost of SOFCs. Beside cost reduction, durability is the most important issue to be solved before any fuel cell technologies can be commercially successful. The durability of a SOFC or stack is affected by many internal and external factors, such as cell design, materials degradation, operational conditions, fuel choice, thermal cycling

and impurities or contaminants. The performance degradation may not avoidable, but can be minimized through a comprehensive understanding of degradation and failure mechanisms and development of appropriate solutions. It is evident that current understanding of these mechanisms on fuel cell components and particularly on the stack level is far from sufficient. Development of new characterization techniques, especially those which allow in situ and quantitative measurements in the atomic level [130-131], and of advanced computational modeling is critical for the quantum leap in understanding of the fundamental issues.

The challenge of meeting the world's gigantic energy demands in a sustainable manner with low environmental impact is undoubtedly one of the most important challenges of this century. IT-SOFC as the most efficient energy conversion technologies should be a technology of choice and can play a critical role to our current and future energy solutions.

Acknowledgment

The financial support by Australia Research Council under contract LP110200281 and National Natural Science Foundation of China (U1134001) is greatly acknowledged.

References:

[1] Jacobson A J. Materials for solid oxide fuel cells [J]. Chemistry of Materials, 2010, 22: 660-674.

[2] Brett D J L, Atkinson A, Brandon N P, et al.Intermicate temperature solid oxide fuel cells [J]. Chemical Society Reviews, 2008, 37: 1568-1578.

[3] Jiang S P, Chan S H. A review of anode materials development in solid oxide fuel cells [J]. Journal of Materials Science, 2004, 39: 4405-4439.

[4] Muller A C, Herbstritt D, Ivers-Tiffee E. Development of a multilayer anode for solid oxide fuel cells [J]. Solid State Ionics, 2002, 152-153: 537-542.

[5] Dees D W, Claar T D, Easler T E, et al. Conductivity of porous Ni/ZrO_2-Y_2O_3 cermets [J]. Journal of the Electrochemical Society, 1987, 134: 2141-2146.

[6] Murray E P, Tsai T, Barnett S A. A direct-methane fuel cell with a ceria-based anode [J]. Na ture, 1999, 400: 649-651.

[7] Tsoga A, Naoumidis A, Nikolopoulos P. Wettability and interfacial reactions in the systems Ni/YSZ and Ni/Ti-TiO_2/YSZ[J]. Acta Materialia, 1996, 44: 3679-3692.

[8] Jiang S P. Sintering behavior of Ni/Y_2O_3-ZrO_2 cermet electrodes of solid oxide fuel cells [J]. Journal of Materials Science, 2003, 38: 3775-3782.

[9] Wilson J R, Kobsiriphat W, Mendoza R, et al. Three-dimensional reconstruction of a solid-oxide fuel-cell anode[J]. Nature Materials, 2006, 5: 541-544.

[10] Chen H Y, Yu H C, Cronin J S, et al. Simulation of coarsening in three-phase solid oxide fuel cell anodes [J]. Journal of Power Sources, 2011, 196: 1333-1337.

[11] Zha S W, Cheng Z, Liu M L. Sulfur poisoning and regeneration of Ni-based anodes in solid oxide fuel cells[J]. Journal of the Electrochemical Society, 2007, 154: B201-B206.

[12] Eguchi K, Kojo H, Takeguchi T, et al. Fuel flexibility in power generation by solid oxide fuel cells[J]. Solid State Ionics, 2002, 152: 411-416.

[13] Kim H, da Rosa C, Boaro M, et al. Fabrication of highly porous yttria-stabilized zirconia by acid leaching nickel from a nickel-yttria-stabilized zirconia cermet[J]. Journal of the American Ceramic Society, 2002, 85: 1473-1476.

[14] Kim H, Lu C, Worrell W L, et al. Cu-Ni cermet anodes for direct oxidation of methane in solid-oxide fuel cells [J]. Journal of the Electrochemical Society, 2002, 149: A247-A250.

[15] Zha S, Tsang P, Cheng Z, et al. Electrical properties and sulfur tolerance of $La_{0.75}Sr_{0.25}Cr_{1-x}Mn_xO_3$ under anodic conditions[J]. Journal of Solid State Chemistry, 2005, 178: 1844-1850.

[16] Mukundan R, Brosha E L, Garzon F H. Sulfur Tolerant Anodes for SOFCs[J]. Electrochemical and Solid-State Letters, 2004, 7: A5-A7.

[17] Aguilar L, Zha S, Li S, et al. Sulfur-tolerant materials for the hydrogen sulfide SOFC[J]. Electrochemical and Solid-State Letters, 2004, 7: A324-A326.

[18] Marina O A, Pederson L R. Novel ceramic anodes for SOFCs tolerant to oxygen, carbon and sulfur, in The Fifth European Solid Oxide Fuel Cell Forum [M]//J Huijismans. European Fuel Cell Forum. Switzerland: Lucerne, 2002: 481-489.

[19] Yang C H, Yang Z B, Jin C, et al. Sulfur-tolerant redox-reversible anode material for direct hydrocarbon solid oxide fuel cells[J]. Advanced Materials, 2012, 24: 1439-1443.

[20] Jiang S P, Chen X J, Chan S H, et al. ($La_{0.75}Sr_{0.25}$)($Cr_{0.5}Mn_{0.5}$)O_3/YSZ composite anodes for methane oxidation reaction in solid oxide fuel cells[J]. Solid State Ionics, 2006, 177: 149-157.

[21] Ong K P, Wu P, Liu L, et al. Optimization of electrical conductivity of $LaCrO_3$ through doping: A combined study of molecular modeling and experiment [J]. Applied Physics Letters, 2007, 90.

[22] Tao S W, Irvine J T S. Synthesis and characterization of ($La_{0.75}Sr_{0.25}$)$Cr_{0.5}Mn_{0.5}O_{3-\delta}$, a redox-stable, efficient perovskite anode for SOFCs[J]. Journal of the Electrochemical Society, 2004, 151: A252-A259.

[23] Jiang S P, Love J G, Apateanu L. Effect of contact between electrode and current collector on the performance of solid oxide fuel cells[J]. Solid State Ionics, 2003, 160: 15-26.

[24] Trembly J P, Marquez A I, Ohrn TR, et al. Effects of coal syngas and H_2S on the performance of solid oxide fuel cells: Single-cell tests[J]. Journal of Power Sources, 2006, 158: 263-273.

[25] Zhang L, Jiang S P, He H Q, et al. A comparative study of H_2S poisoning on electrode behavior of Ni/YSZ and Ni/GDC anodes of solid oxide fuel cells[J]. International Journal of Hydrogen Energy, 2010, 35: 12359-12368.

[26] Kerman K, Lai B K, Ramanathan S. Pt/$Y_{0.16}Zr_{0.84}O_{1.92}$/Pt thin film solid oxide fuel cells: Electrode microstructure and stability considerations[J]. Journal of Power Sources, 2011, 196: 2608-2614.

[27] Ye Y M, He T M, Li Y, et al. Pd-promoted $La_{0.75}Sr_{0.25}Cr_{0.5}Mn_{0.5}O_3$/YSZ composite anodes for direct utilization of methane in SOFCs[J]. Journal of the Electrochemical Society, 2008, 155: B811-B818.

[28] Klages M, Kruger P, Haussmann J, et al. Investigation of the influence of GDL properties on the water balance by means of neutron radiography[J]. Materials Testing, 2010, 52: 718-724.

[29] Jin Y, Yasutake H, Yamahara K, et al. Suppressed carbon deposition behavior in nickel/yittria-stablized zirconia anode with $SrZr_{0.95}Y_{0.05}O_{3-\alpha}$ in dry methane fuel [J]. Journal of the Electrochemical Society, 2010, 157: B130-B134.

[30] Wang W, Jiang S P, Tok A I Y, et al. GDC-impregnated Ni anodes for direct utilization of methane in solid oxide fuel cells[J]. Journal of Power Sources, 2006, 159: 68-72.

[31] Yang L, Choi Y, Qin W T, et al. Promotion of water-mediated carbon removal by nanostructured barium oxide/nickel interfaces in solid oxide fuel cells [J]. Nature Communications, 2011, 2.

[32] Cheng Z, Wang J H, Choi Y M, et al. From Ni-YSZ to sulfur-tolerant anode materials for SOFCs: Electrochemical behavior, in situ characterization, modeling, and future perspectives[J]. Energy & Environmental Science, 2011, 4: 4380-4409.

[33] Jiang S P. Development of lanthanum strontium manganite perovskite cathode materials of solid oxide fuel cells: A review[J]. Journal of Materials Science, 2008, 43: 6799-6833.

[34] Carter S, Selcuk A, Chater R J, et al. Oxygen-transport in selected nonstoichiometric perovskite-structure oxides[J]. Solid State Ionics, 1992, 53-56: 597-605.

[35] Zhen Y D, Jiang S P. Transition behavior for O_2 reduction reaction on (La,Sr)MnO_3/YSZ composite cathodes of solid oxide fuel cells[J]. Journal of the Electrochemical Society, 2006, 153: A2245-A2254.

[36] Jiang S P, Wang W. Fabrication and performance of GDC-impregnated (La,Sr)MnO_3 cathodes for intermediate temperature solid oxide fuel cells[J]. Journal of the Electrochemical Society, 2005, 152: A1398-A1408.

[37] Esquirol A, Brandon N P, Kilner J A, et al. Electrochemical characterization of $La_{0.6}Sr_{0.4}Co_{0.2}Fe_{0.8}O_3$ cathodes for intermediate-temperature SOFCs[J]. Journal of the Electrochemical Society, 2004, 151: A1847-A1855.

[38] Jiang S P. A comparison of O_2 reduction reactions on porous (La,Sr)MnO_3 and (La,Sr)(Co,Fe)O_3 electrodes [J]. Solid State Ionics, 2002, 146: 1-22.

[39] Shao Z P, Haile S M. A high-performance cathode for the next generation of solid-oxide fuel cells[J]. Nature, 2004, 431: 170-173.

[40] Wei B, Lu Z, Li S Y, et al. Thermal and electrical properties of new cathode material $Ba_{0.5}Sr_{0.5}Co_{0.8}Fe_{0.2}O_{3-\delta}$ for solid oxide fuel cells[J]. Electrochemical and Solid State Letters, 2005, 8: A428-A431.

[41] Yi J X, Schroeder M, Weirich T, et al. Behavior of Ba(Co, Fe, Nb)$O_{3-\delta}$ perovskite in CO_2-containing atmospheres: Degradation mechanism and materials design [J]. Chemistry of Materials, 2010, 22: 6246-6253.

[42] Zhou W, Liang F L, Shao Z P, et al. Hierarchical CO_2-protective shell for highly efficient oxygen reduction reaction[J]. Scientific Reports, 2012, 2.

[43] Tu H Y, Stimming U. Advances, aging mechanisms and lifetime in solid-oxide fuel cells[J]. Journal of Power Sources, 2004, 127: 284-293.

[44] Fergus J W. Effect of cathode and electrolyte transport properties on chromium poisoning in solid oxide fuel

cells [J]. International Journal of Hydrogen Energy, 2007, 32: 3664-3671.

[45] Schuler J A, Gehrig C, Wuillemin Z, et al. Air side contamination in solid oxide fuel cell stack testing[J]. Journal of Power Sources, 2011, 196: 7225-7231.

[46] Taniguchi S, Kadowaki M, Yasuo T, et al. Suppression of chromium diffusion to an SOFC cathode from an alloy separator by a cathode second layer [J]. Denki Kagaku, 1996, 64: 568-574.

[47] Fu C J, Sun K N, Zhang N Q, et al. Mechanism of chromium poisoning of LSM cathode in solid oxide fuel cell [J]. Chemical Journal of Chinese Universities-Chinese, 2007, 28: 1762-1764.

[48] Konysheva E, Penkalla H, Wessel E, et al. Chromium poisoning of perovskite cathodes by the ODS alloy $Cr5Fe1Y_2O_3$ and the high chromium ferritic steel Crofer22APU[J]. Journal of the Electrochemical Society, 2006, 153: A765-A773.

[49] Paulson S C, Birss V I. Chromium poisoning of LSM-YSZ SOFC cathodes - I. Detailed study of the distribution of chromium species at a porous, single-phase cathode [J]. Journal of the Electrochemical Society, 2004, 151: A1961-A1968.

[50] Jiang S P, Zhang J P, Apateanu L, et al. Deposition of chromium species at Sr-doped $LaMnO_3$ electrodes in solid oxide fuel cells I. Mechanism and kinetics [J]. Journal of the Electrochemical Society, 2000, 147: 4013-4022.

[51] Badwal S P S, Deller R, Foger K, et al. Interaction between chromia forming alloy interconnects and air electrode of solid oxide fuel cells [J]. Solid State Ionics, 1997, 99: 297-310.

[52] Jiang S P, Christiansen L, Hughan B, et al. Effect of glass sealant materials on microstructure and performance of Sr-doped $LaMnO_3$ cathodes[J]. Journal of Materials Science Letters, 2001, 20: 695-697.

[53] Xiong Y P, Yamaji K, Horita T, et al. Sulfur Poisoning of SOFC Cathodes[J]. Journal of the Electrochemical Society, 2009, 156: B588-B592.

[54] Horita T, Kishimoto H, Yamaji K, et al. Effects of impurities on the degradation and long-term stability for solid oxide fuel cells[J]. Journal of Power Sources, 2009, 193: 194-198.

[55] Zhou X D, Templeton J W, Zhu Z, et al. Electrochemical performance and stability of the cathode for solid oxide fuel cells[J]. Journal of the Electrochemical Society, 2010, 157: B1019-B1023.

[56] Jiang S P. Nanoscale and nano-structured electrodes of solid oxide fuel cells by infiltration: Advances and challenges [J]. International Journal of Hydrogen Energy, 2012, 37: 449-470.

[57] Gorte R J, Vohs J M. Nanostructured anodes for solid oxide fuel cells[J]. Current Opinion in Colloid & Interface Science, 2009, 14: 236-244.

[58] Jiang Z Y, Xia C R, Chen F L. Nano-structured composite cathodes for intermediate-temperature solid oxide fuel cells via an infiltration/impregnation technique [J]. Electrochimica Acta, 2010, 55: 3595-3605.

[59] Sholklapper T Z, Jacobson C P, Visco S J, et al. Synthesis of dispersed and contiguous nanoparticles in solid oxide fuel cell electrodes[J]. Fuel Cells, 2008, 8: 303-312.

[60] Liang F L, Chen J, Cheng J L, et al. Novel nano-structured Pd plus yttrium doped ZrO_2 cathodes for intermediate temperature solid oxide fuel cells [J]. Electrochemistry Communications, 2008, 10: 42-46.

[61] Sholklapper T Z, Kurokawa H, Jacobson C P, et al. Nanostructured solid oxide fuel cell electrodes[J]. Nano Letters, 2007, 7: 2136-2141.

[62] Jung S W, Vohs J M, Gorte R J. Preparation of SOFC anodes by electrodeposition[J]. Journal of the Electrochemical Society, 2007, 154: B1270-B1275.

[63] Ai N, Jiang S P, Chen K F, et al. Vacuum-assisted electroless copper plating on Ni/$(Sm,Ce)O_2$ anodes for intermediate temperature solid oxide fuel cells[J]. International Journal of Hydrogen Energy, 2011, 36: 7661-7669.

[64] Jiang S P, Wang W. Novel structured mixed ionic and electronic conducting cathodes of solid oxide fuel cells [J]. Solid State Ionics, 2005, 176: 1351-357.

[65] Murray E P, Barnett S A. (La,Sr) MnO_3-$(Ce,Gd)O_{2-x}$ composite cathodes for solid oxide fuel cells[J]. Solid State Ionics, 2001, 143: 265-273.

[66] Jiang S P, Zhang J P, Foger K. Deposition of chromium species at Sr-doped $LaMnO_3$ electrodes in solid oxide fuel cells - II. Effect on O_2 reduction reaction[J]. Journal of the Electrochemical Society, 2000, 147: 3195-3205.

[67] Murray E P, Tsai T, Barnett S A. Oxygen transfer processes in $(La,Sr)MnO_3/Y_2O_3$-stabilized ZrO_2 cathodes: an impedance spectroscopy study[J]. Solid State Ionics, 1998, 110: 235-243.

[68] Ai N, Jiang S P, Lu Z, et al. Nanostructured $(Ba,Sr)(Co,Fe)O_{3-\delta}$ impregnated $(La,Sr)MnO_3$ cathode for intermediate-temperature solid oxide fuel cells [J]. Journal of the Electrochemical Society, 2010, 157: B1033-B1039.

[69] Shah M, Voorhees P W, Barnett S A. Time-dependent

performance changes in LSCF-infiltrated SOFC cathodes: The role of nano-particle coarsening[J]. Solid State Ionics, 2011, 187: 64-67.

[70] Liang F L, Chen J, Jiang S P, et al. Mn-stabilised microstructure and performance of Pd-impregnated YSZ cathode for intermediate temperature solid oxide fuel cells[J]. Fuel Cells, 2009, 9: 636-642.

[71] Babaei A, Zhang L, Liu E J, et al. Performance and stability of $La_{0.8}Sr_{0.2}MnO_3$ cathode promoted with palladium based catalysts in solid oxide fuel cells [J].Journal of Alloys and Compounds, 2011, 509: 4781-4787.

[72] Badwal S P S. Zirconia-based solid electrolytes-microstructure, stability and ionic-conductivity [J]. Solid State Ionics, 1992, 52: 23-32.

[73] Ishihara T. Development of new fast oxide ion conductor and application for intermediate temperature solid oxide fuel cells [J]. Bulletin of the Chemical Society of Japan, 2006, 79: 1155-1166.

[74] Hull S. Superionics: Crystal structures and conduction processes [J]. Reports on Progress in Physics, 2004, 67: 1233-1314.

[75] Nomura K, Mizutani Y, Kawai M, et al. Aging and Raman scattering study of scandia and yttria doped zirconia[J]. Solid State Ionics, 2000, 132: 235-239.

[76] Badwal S P S, Ciacchi F T, Rajendran S, et al. An investigation of conductivity, microstructure and stability of electrolyte compositions in the system 9 mol% (Sc_2O_3-Y_2O_3)-ZrO_2(Al_2O_3)[J]. Solid State Ionics, 1998, 109: 167-186.

[77] Badwal S P S, Rajendran S. Effect of microstructures and nanostructures on the properties of ionic conductors[J]. Solid State Ionics, 1994, 70: 83-95.

[78] Liu Y, Lao L E. Structural and electrical properties of ZnO-doped 8 mol% yttria-stabilized zirconia[J]. Solid State Ionics, 2006, 177: 159-163.

[79] Mogensen M, Sammes N M, Tompsett G A. Physical, chemical and electrochemical properties of pure and doped ceria[J]. Solid State Ionics, 2000, 129: 63-94.

[80] Zhan Z L, Wen T L, Tu H Y, et al. AC impedance investigation of samarium-doped ceria [J]. Journal of the Electrochemical Society, 2001, 148: A427-A432.

[81] Jung G B, Huang T J, Chang C L. Effect of temperature and dopant concentration on the conductivity of samaria-doped ceria electrolyte[J]. Journal of Solid State Electrochemistry, 2002, 6: 225-230.

[82] Zha S W, Xia C R, Meng G Y. Effect of Gd (Sm) doping on properties of ceria electrolyte for solid oxide fuel cells[J]. Journal of Power Sources, 2003, 115: 44-48.

[83] Vanherle J, Horita T, Kawada T, et al. Sintering behaviour and ionic conductivity of yttria-doped ceria[J]. Journal of the European Ceramic Society, 1996, 16: 961-973.

[84] Zhang X, Robertson M, Deces-Petit C, et al. Internal shorting and fuel loss of a low temperature solid oxide fuel cell with SDC electrolyte [J]. Journal of Power Sources, 2007, 164: 668-677.

[85] Ishihara T, Tabuchi J, Ishikawa S, et al. Recent progress in $LaGaO_3$ based solid electrolyte for intermediate temperature SOFCs [J]. Solid State Ionics, 2006, 177: 1949-1953.

[86] Yan J W, Matsumoto H, Enoki M, et al. High-power SOFC using $La_{0.9}Sr_{0.1}Ga_{0.8}Mg_{0.2}O_{3-\delta}$/$Ce_{0.8}Sm_{0.2}O_{2-\delta}$ composite film [J]. Electrochemical and Solid State Letters, 2005, 8: A389-A391.

[87] Kosacki I, Rouleau C M, Becher P F, et al. Nanoscale effects on the ionic conductivity in highly textured YSZ thin films[J]. Solid State Ionics, 2005, 176: 1319-1326.

[88] Garcia-Barriocanal J, Rivera-Calzada A, Varela M, et al. Colossal ionic conductivity at interfaces of epitaxial ZrO_2 : Y_2O_3/$SrTiO_3$ heterostructures [J]. Science, 2008, 321: 676-680.

[89] Vincent A, Savignat S B, Gervais F. Elaboration and ionic conduction of apatite-type lanthanum silicates doped with Ba, $La_{10-x}Bax(SiO_4)$ $6O_{3-x/2}$ with x=0.25-2[J]. Journal of the European Ceramic Society, 2007, 27: 1187-1192.

[90] Slater P R, Sansom J E H, Tolchard J R. Development of apatite-type oxide ion conductors[J]. Chemical Record, 2004, 4: 373-384.

[91] Jiang S P, Zhang L, He H Q, et al. Synthesis and characterization of lanthanum silicate apatite by gel-casting route as electrolytes for solid oxide fuel cells[J]. Journal of Power Sources, 2009, 189: 972-981.

[92] Komori S, Kimura M, Watanabe K, et al. Compact fuel processor by employing monolithic catalyst for 1 kW class residential polymer electrolyte fuel cells[J]. Journal of the Japan Petroleum Institute, 2011, 54: 52-5.

[93] Jung D W, Duncan K L, Wachsman E D. Effect of total dopant concentration and dopant ratio on conductivity of $(D_yO_{1.5})_x$-$(WO_3)_y$-$(BiO_{1.5})_{1-x-y}$[J]. Acta Materialia, 2010, 58: 355-363.

[94] Wachsman E D, Jayaweera P, Jiang N, et al. Stable high conductivity ceria/bismuth oxide bilayered electrolytes [J]. Journal of the Electrochemical Society, 1997, 144: 233-236.

[95] Ahn J S, Pergolesi D, Camaratta M A, et al. High-per-

formance bilayered electrolyte intermediate temperature solid oxide fuel cells[J]. Electrochemistry Communications, 2009, 11: 1504-1507.

[96] Mori M, Yamamoto T, Itoh H, et al. Compatibility of alkaline earth metal (Mg, Ca, Sr)-doped lanthanum chromites as separators in planar-type high-temperature solid oxide fuel cells [J]. Journal of Materials Science, 1997, 32: 2423-2431.

[97] Fergus J W. Lanthanum chromite-based materials for solid oxide fuel cell interconnects[J]. Solid State Ionics, 2004, 171: 1-15.

[98] Sakai N, Yokokawa H, Horita T, et al. Lanthanum chromite-based interconnects as key materials for SOFC stack development[J]. International Journal of Applied Ceramic Technology, 2004, 1: 23-30.

[99] Liu Z G, Zheng Z R, Huang X Q, et al. The Pr^{4+} ions in Mg doped $PrGaO_3$ perovskites[J]. Journal of Alloys and Compounds, 2004, 363: 60-62.

[100] Zhou X L, Deng F J, Zhu M X, et al. High performance composite interconnect $La_{0.7}Ca_{0.3}CrO_{3/20}$ mol% $ReO_{1.5}$ doped CeO_2 (Re = Sm, Gd, Y) for solid oxide fuel cells[J]. Journal of Power Sources, 2007, 164: 293- 299.

[101] Shen Y, Liu M N, He T M, et al. A potential interconnect material for solid oxide fuel cells: $Nd_{0.75}Ca_{0.25}Cr_{0.98}O_{3-\delta}$ [J]. Journal of Power Sources, 195: 977-983.

[102] Zhu W Z, Deevi S C. Development of interconnect materials for solid oxide fuel cells [J]. Materials Science and Engineering A-Structural Materials Properties Microstructure and Processing, 2003, 348: 227-243.

[103] Fergus J W. Metallic interconnects for solid oxide fuel cells[J]. Materials Science and Engineering A-Structural Materials Properties Microstructure and Processing, 2005, 397: 271-283.

[104] Holt A, Kofstad P. Electrical-conductivity and derect structure of Cr_2O_3. 2. Reduced temperatures (less than similar to 1000 °C)[J]. Solid State Ionics, 1994, 69: 137-143.

[105] Quadakkers W J, Hansel M, Rieck T. Carburization of Cr-based ODS alloys in SOFC relevant environments [J]. Materials and Corrosion-Werkstoffe Und Korrosion, 1998, 49: 252-257.

[106] Blum L, Buchkremer H P, Gross S, et al. Solid oxide fuel cell development at Forschungszentrum Juelich [J]. Fuel Cells, 2007, 7: 204-210.

[107] Yang Z G, Hardy J S, Walker M S, et al. Structure and conductivity of thermally grown scales on ferritic Fe-Cr-Mn steel for SOFC interconnect applications[J]. Journal of the Electrochemical Society, 2004, 151: A1825-A1831.

[108] Yao K S, Chen Y C, Chao C H, et al. Electrical enhancement of DMFC by Pt-M/C catalyst-assisted PVD[J]. Thin Solid Films, 2010, 518: 7225-7228.

[109] Hua B, Pu J, Zhang J F, et al. Ni-Mo-Cr alloy for interconnect applications in intermediate temperature solid oxide fuel cells[J]. Journal of the Electrochemical Society, 2009, 156: B93-B98.

[110] Chen X B, Hua B, Pu J, et al. Interaction between (La, Sr)MnO_3 cathode and Ni-Mo-Cr metallic interconnect with suppressed chromium vaporization for solid oxide fuel cells[J]. International Journal of Hydrogen Energy, 2009, 34: 5737-5748.

[111] Fergus J W. Sealants for solid oxide fuel cells[J]. Journal of Power Sources, 2005, 147: 46-57.

[112] Eichler K, Solow G, Otschik P, et al. BAS ($BaO \cdot Al_2O_3 \cdot SiO_2$)-glasses for high temperature applications [J]. Journal of the European Ceramic Society, 1999, 19: 1101-1104.

[113] Yang Z G, Stevenson J W, Meinhardt K D. Chemical interactions of barium-calcium-aluminosilicate-based sealing glasses with oxidation resistant alloys[J]. Solid State Ionics, 2003, 160: 213-225.

[114] Chen K F, Ai N, Lievens C, et al. Impact of volatile boron species on the microstructure and performance of nano-structured $(Gd,Ce)O_2$ infiltrated (La,Sr)MnO_3 cathodes of solid oxide fuel cells[J]. Electrochemistry Communications, 2012: in press.

[115] Duquette J, Petric A. Silver wire seal design for planar solid oxide fuel cell stack[J]. Journal of Power Sources, 2004, 137: 71-75.

[116] Bram M, Reckers S, Drinovac P, et al. Deformation behavior and leakage tests of alternate sealing materials for SOFC stacks[J]. Journal of Power Sources, 2004, 138: 111-119.

[117] Sang S B, Pu J, Jiang S P, et al. Prediction of H_2 leak rate in mica-based seals of planar solid oxide fuel cells[J]. Journal of Power Sources, 2008, 182: 141-144.

[118] Chou Y S, Stevenson J W, Chick L A. Ultra-low leak rate of hybrid compressive mica seals for solid oxide fuel cells[J]. Journal of Power Sources, 2002, 112: 130-136.

[119] Chou Y S, Stevenson J W. Thermal cycling and degradation mechanisms of compressive mica-based seals

for solid oxide fuel cells[J]. Journal of Power Sources, 2002, 112: 376-383.

[120] Khan T I, Al-Badri A. Reactive brazing of ceria to an ODS ferritic stainless steel[J]. Journal of Materials Science, 2003, 38: 2483-8.

[121] Weil K S. The state-of-the-art in sealing technology for solid oxide fuel cells[J]. Jom, 2006, 58: 37-44.

[122] Foger K, Love J G. Fifteen years of SOFC development in Australia[J]. Solid State Ionics, 2004, 174: 119-126.

[123] Jiang S P. Thin coating technologies and applications in high-temperature solid oxide fuel cells[M]// Zhang S. Handbook of nanostructured film devices and coatings. CRC Press, 2010: 155-187.

[124] Minh N Q. Solid oxide fuel cell technology-features and applications[J]. Solid State Ionics, 2004, 174: 271-277.

[125] Srivastava P K, Quach T, Duan Y Y, et al. Electrode supported solid oxide fuel cells: Electrolyte films prepared by DC magnetron sputtering[J]. Solid State Ionics, 1997, 99: 311-319.

[126] Kim J W, Virkar A V, Fung K Z, et al. Polarization effects in intermediate temperature, anode-supported solid oxide fuel cells[J]. Journal of the Electrochemical Society, 1999, 146: 69-78.

[127] Sarantaridis D, Atkinson A. Redox cycling of Ni-based solid oxide fuel cell anodes: A review[J]. Fuel Cells, 2007, 7: 246-58.

[128] Lang M, Henne R, Schaper S, et al. Development and characterization of vacuum plasma sprayed thin film solid oxide fuel cells[J]. Journal of Thermal Spray Technology, 2001, 10: 618-625.

[129] Brandon N P, Blake A, Corcoran D, et al. Development of metal supported solid oxide fuel cells for operation at 500-600 °C[J]. Journal of Fuel Cell Science and Technology, 2004, 1: 61-65.

[130] Bryant B, Renner C, Tokunaga Y, et al. Imaging oxygen defects and their motion at a manganite surface [J]. Nature Communications, 2011, 2.

[131] Cheng Z, Liu M L. Characterization of sulfur poisoning of Ni-YSZ anodes for solid oxide fuel cells using in situ Raman micro spectroscopy[J]. Solid State Ionics, 2007, 178: 925-935.

中温固体氧化物燃料电池优势和挑战的简要评述

蒋三平

(科廷大学 燃料与能源技术研究院，化学工程系，澳大利亚 西澳省珀斯 6102)

摘要：燃料电池是一种将燃料的化学能直接转化为电能的电化学发电装置. 在各种类型的燃料电池中，固体氧化物燃料电池(SOFC)在 600～800 °C 的中温区运行，因此与质子交换膜燃料电池等低温燃料电池相比，其燃料选择范围更广，具有更广泛的应用前景. 然而，SOFC 的商业应用面临着两大挑战：成本和稳定性. 这两种挑战与阳极、阴极、电解质、连接体和密封材料等组件的加工、制备、性能、化学和微结构稳定性密切相关. 电池堆的导管连接材料也需要经过仔细地筛选，以最大限度地降低有毒害的挥发性成分，从而确保电池结构的稳定和完整. 本文旨在简要评述 SOFC 的材料和组分的研究现状，并提出展望. 同时，对新一代 SOFC 技术面临的机遇和挑战进行了探讨.

关键词：中温固体氧化物燃料电池；评述；挑战；材料